

First-principles calculations of optical properties: Application to silicon clusters

Cecilia Noguez*

Instituto de Física, Universidad Nacional Autónoma de México, Apartado Postal 20-364, México, Distrito Federal 01000, Mexico

Sergio E. Ulloa

Department of Physics and Astronomy, and Condensed Matter and Surface Sciences Program, Ohio University, Athens, Ohio 4570-2979

(Received 19 May 1997)

We have developed an *ab initio* method to calculate optical properties of crystals, clusters, and surfaces starting from their fully relaxed atomic configurations. The approach allows dealing with systems consisting of up to several hundred atoms per unit cell. We present results for silicon clusters consisting of 20, 60, and 70 atoms. We calculate the optical dielectric response function for clusters with different atomic structure. Quantum molecular dynamics simulations were performed to find metastable and equilibrium (lowest-energy) atomic configurations. We discuss the dependence of the optical properties of these silicon clusters on the number of atoms as well as on the specific structural properties. Comparison with theoretical and experimental results is also presented. [S0163-1829(97)01239-3]

I. INTRODUCTION

The continuing development of materials growth and nanostructure technologies makes evident the need for detailed theoretical understanding of these systems. Several theoretical approximations have been developed to study their basic properties. Most of these methods provide excellent information on the ground state, although the *ab initio* methods demand typically a substantial computational effort. These methods are then limited to study systems with a somewhat small number of atoms, and only a few calculations of excited properties have been performed.

The study of excitations in systems, such as those measured by optical experiments are even more difficult to achieve: (i) The computational effort is much larger, since it requires calculation of additional matrix elements, and (ii) it is absolutely necessary to have a good *microscopic* description of the single-particle-like electronic states; not only of the filled “valence” electronic states, but also of the empty “conduction” states near the main energy gap in semiconductors and insulators. These two facts have contributed, in great part, to limit such kind of calculations, and have limited even more the number of atoms per unit cell used in the description of these systems.

Here we present a method that employs a localized pseudoatomic orbital basis set that allows one to calculate optical properties of systems with as many as a few hundred atoms. The choice of this basis set results in calculations that are much more convenient than traditional *ab initio* methods, based on plane-wave basis sets,¹ in the study of semiconductor clusters and surfaces. However, some attempts to calculate optical properties of surfaces have been made.^{2,3} The use of localized wave functions reduces the number of calculations needed to compute, for example, the long-wavelength dielectric function, $\epsilon(\omega)$, as we will describe below.

Typically, plane-waves *ab initio* methods have been used to carry out quantum molecular dynamics (QMD) calculations. These methods, although powerful and versatile, re-

quire thousands of plane waves to correctly compute the valence and conduction bands of systems with a few tens of atoms. In our case, the localized basis set employs a number of wave functions equal to the number of local set functions times the total number of atoms per unit cell. For example, while in the largest cluster studied here it is necessary to employ about 20 000 plane waves, in our method we use only 630 localized wave functions (=nine localized orbitals per atom \times 70 atoms). We have applied this scheme to calculate the electronic and optical properties of silicon clusters consisting of 20, 60, and 70 atoms. We will discuss below the results of these calculations.

Silicon clusters of small and intermediate size have received a great deal of attention.⁴⁻⁸ One of the reasons, apart from possible future technological applications in optoelectronics, is perhaps that silicon clusters do not show equilibrium symmetric fullerene structures like carbon, but rather exhibit more compact geometries which favor fourfold bondings. This behavior has been attributed to the different competition between structure (strains) and electronic properties (bonding) involved in the equilibration process. Moreover, silicon clusters may be important in understanding the bright photoluminescence properties found in porous silicon. Normally, photoluminescence from bulk Si is quite weak due to the indirect nature of the fundamental gap. The “anomalous” behavior seen in porous Si has been attributed to quantum confinement of electrons and/or surface effects. However, the role played by size confinement and surfaces with dangling bond effects is not completely understood.⁹ On the other hand, some resemblance between porous silicon and small and intermediate clusters has been found.⁶

A few theoretical efforts to understand silicon clusters have been reported, where equilibrium structures of these systems have been carefully studied.^{4,5} However, the computational limitations mentioned above have perhaps hampered the theoretical study of optical properties in these clusters. On the other hand, experimental characterization using traditional techniques, such as x rays, is difficult to perform due

to the small size of these systems, suggesting as an important alternative the use of optical techniques. However, the determination of optical properties of clusters from first-principles calculations is needed, if one is to compare with experiments. It is to this end that we have focused our efforts. We should note, however, that recent interesting developments in the theoretical determination of optical properties of surfaces starting from structures obtained using plane-waves approaches have also appeared in the literature.¹⁰

We present here a first-principles computational scheme to calculate the optical properties of clusters and other systems. We apply this scheme to calculate the electronic and optical properties of silicon clusters with small and intermediate sizes. The approach presented here not only provides a method to calculate optical properties, but also answers some fundamental questions about the overall behavior of silicon nanostructures. We find that as the number of atoms in the cluster increases, the energy (optical) gap decreases, due mostly to the decreasing influence of quantum confinement on the electronic states. We find, moreover, that the geometry and consequent electronic levels of a cluster have important consequences on the optical properties. Despite different number of atoms, the observed optical response is fairly isotropic, with some exceptions. These general results prove that one should be able to correlate the observed optical absorption spectrum with the calculated atomic structure. This is especially true if different metastable configurations are allowed during the fabrication stages of clusters. The calculated geometry and optical absorption spectra should aid the identification of such cluster systems, when other traditional characterization techniques are not applicable or hard to implement.

This manuscript has been organized as follows. In Sec. II, we explain the computational details and approximations used to calculate the optical properties. In Sec. III, we explain the atomic models of clusters, and discuss the calculated electronic and optical responses. The discussion is made in terms of the number of atoms, and the different stable and metastable structures. Finally, our conclusions are presented in Sec. IV.

II. METHODOLOGY

This section has been divided in two. We first briefly explain the computational method used to perform the QMD calculation. In the second part, we explain the method and approximations used to calculate the optical properties within our QMD scheme.

A. Computational method

The approach used here is a QMD based in a first-principles method developed by Sankey and Niklewski.¹¹ This scheme is based on density functional theory in the local density approximation (LDA), using Harris functionals, the Hamann-Schlüter-Chiang pseudopotentials,¹² and a minimal sp^3 basis representation. A comprehensive discussion of this scheme, approximations used, and a description of various tests can be found in Ref. 13.

In particular, this method has been shown to be very useful in the description of small and large silicon systems, including the π -bonded (2×1) reconstruction of the (111) sur-

face, the 2×1 , $p(2 \times 2)$, and $c(4 \times 2)$ phases of the (100) surfaces, the 5×5 reconstruction of Si(111), as well as kinetic processes like the hydrogenation of the large 7×7 -(111) surface.¹³⁻¹⁵ This computational technique does not involve fitting parameters like semiempirical approaches, and yields very accurate results. It has been shown to be quite reliable and its execution time is moderate compared with other *ab initio* methods. Moreover, the use of a localized basis set is more convenient to study clusters than other methods using plane-wave basis sets.

Initial and relaxed atomic geometries. Our starting point for the QMD are the ideal cluster structures that resemble the corresponding carbon fullerenes C_n ($n = 20, 60,$ and 70), but are properly scaled to the Si-Si bonding environment (i.e., the bond length in each structure is chosen to minimize the total energy, while keeping the fullerene geometry). We study then the metastable and equilibrium geometries of silicon clusters that are obtained after annealing and quenching such ideal clusters.^{5,11} In annealing, the cluster is subjected to large temperatures (few thousands Kelvins) and then the cluster is relaxed for a long period of time (about five picoseconds) to achieve typically a highly disordered structure. Then, the structure is “frozen” or quenched by removing the kinetic energy of the atoms, and further allowed to follow the dynamics dictated by the calculated forces. The repeated quenching stages lead the system to a lower-energy configuration on each step, yielding either metastable structures, or even lower energy or “equilibrium” configurations. A detailed description of the procedure employed to calculate the Si_n atomic configurations used here, as well as their atomic and vibrational characteristic properties, was presented by Song *et al.* in Ref. 5.

B. Linear optical calculations

Once the metastable and equilibrium atomic configurations of the Si_{20} , Si_{60} , and Si_{70} clusters are found, we consider their electronic configurations to calculate the corresponding optical properties. In the calculation of the cluster dielectric function $\epsilon(\omega)$, electronic transitions between filled and empty states must be taken into account. In order to describe as well as possible the valence (v , filled) and conduction (c , empty) bands or levels, we improve the electronic states by performing the first-principles calculations described above but now using an extended basis, where the d atomiclike localized orbitals are included. This extended basis (sp^3d^5) has shown to be very accurate, and compares very well with conventional *ab initio* methods in describing valence and conduction bands of a variety of systems.^{16,17}

The imaginary part of $\epsilon(\omega)$ is calculated within the random phase approximation according to the well-known relation¹⁸

$$\text{Im}[\epsilon^{jj}(\omega)] = \frac{e^2 \hbar^2}{\pi m^2 \omega^2} \sum_{v,c} |\langle \psi_c | \hat{\mathbf{e}}_j \cdot \mathbf{p} | \psi_v \rangle|^2 \delta(E_c - E_v - \hbar \omega), \quad (1)$$

where $\hat{\mathbf{e}}_j$ is a unitary vector along the direction of the external electromagnetic field of energy $\hbar \omega$, \mathbf{p} is the momentum operator, e and m are the charge and mass of the bare elec-

tron, ψ_c and ψ_v are the empty and filled state eigenfunctions of the system, respectively, and E_c and E_v their corresponding energies.

To calculate the optical matrix elements of Eq. (1), $\langle \psi_c | \hat{\mathbf{e}}_j \cdot \mathbf{p} | \psi_v \rangle$, we use the commutation relation between Hamiltonian and position operator,

$$\mathbf{p} = \frac{im}{\hbar} [H, \mathbf{r}] = \frac{im}{\hbar} (H\mathbf{r} - \mathbf{r}H). \quad (2)$$

Using this relation, the matrix elements of the momentum operator between eigenstates are obtained in terms of those between localized orbitals $\phi_{n\mathbf{R}}(\mathbf{r})$, as¹⁸

$$\begin{aligned} \langle \phi_{n\mathbf{R}} | p_j | \phi_{n'\mathbf{R}'} \rangle = & \frac{im}{\hbar} \sum_{n''} \{ \langle \phi_{n\mathbf{R}} | H | \phi_{n''\mathbf{R}''} \rangle \langle \phi_{n''\mathbf{R}''} | r_j | \phi_{n'\mathbf{R}'} \rangle \\ & - \langle \phi_{n\mathbf{R}} | r_j | \phi_{n''\mathbf{R}''} \rangle \langle \phi_{n''\mathbf{R}''} | H | \phi_{n'\mathbf{R}'} \rangle \}. \quad (3) \end{aligned}$$

Here, $p_j \equiv \hat{\mathbf{e}}_j \cdot \mathbf{p}$, and $r_j \equiv \hat{\mathbf{e}}_j \cdot \mathbf{r}$, n denotes the local orbital (or ‘‘momentum’’) index, and \mathbf{R} and \mathbf{R}' are the atomic positions about which the atomiclike orbitals are localized. Finally, we rewrite the matrix elements of the position operator of Eq. (3), such that

$$\begin{aligned} \langle \phi_{n\mathbf{R}} | r_j | \phi_{n'\mathbf{R}'} \rangle = & \frac{1}{2} (R_j + R'_j) \langle \phi_{n\mathbf{R}} | \phi_{n'\mathbf{R}'} \rangle \\ & + \langle \phi_{n\mathbf{R}} | [r_j - \frac{1}{2} (R_j + R'_j)] | \phi_{n'\mathbf{R}'} \rangle. \quad (4) \end{aligned}$$

Notice that the second term on the right-hand side of Eq. (4) is usually assumed small and neglected, and the nonorthogonality of the basis is ignored. In that case, the usual expression for the dipole matrix element is found,

$$\langle \phi_{n\mathbf{R}} | p_j | \phi_{n'\mathbf{R}'} \rangle \approx \frac{im}{\hbar} (R'_j - R_j) \langle \phi_{n\mathbf{R}} | H | \phi_{n'\mathbf{R}'} \rangle. \quad (5)$$

Here, we perform calculations taking into account the non-orthogonality of the basis, and the second term on the right-hand side of Eq. (4) was approximated by considering only intra-atomic transitions—the so-called sp and pd dipoles. Notice that these latter terms become more important when the system studied has dangling bonds, as it is expected in clusters. We have indeed found that the difference between the dipole moment calculated with Eq. (5) and the full equation (3), as described, can be significant in some cases.

To test our method, we first calculate $\epsilon(\omega)$ for bulk silicon.¹⁹ In this case, we have employed the scissors operator to roughly correct the typically underestimated LDA energy gap. This rigidly opens the gap while leaving the wave functions unchanged.²⁰ The imaginary part of $\epsilon(\omega)$ was calculated using a relation similar to Eq. (1),²¹ where the sum over valence and conduction states was averaged over 4648 special points in the irreducible part of the Brillouin zone.²² Electron transitions up to 10 eV were taken into account, to ensure that the real part of $\epsilon(\omega)$, obtained by using the Kramers-Kronig relation, be valid up to about 5 eV. The calculated value of the static dielectric constant $\epsilon(0) = 11.76$, is in excellent agreement with the experimental result of 11.8. The imaginary part of $\epsilon(\omega)$ exhibits electronic transitions starting at about 3 eV, with two main peaks at 3.6 and 4.2 eV. These transitions correspond well to those observed in experiments at 3.4 and 4.5 eV, respectively. The

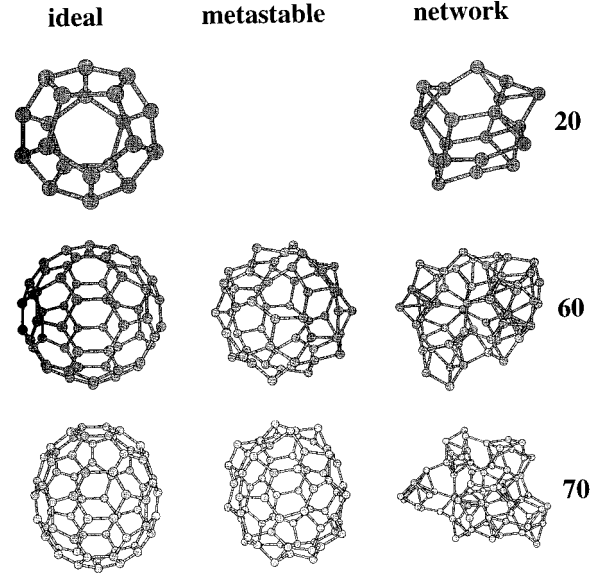


FIG. 1. Atomic structure of ideal, metastable, and equilibrium (lowest energy found) configurations of Si_{20} , Si_{60} , and Si_{70} .

calculated real part of $\epsilon(\omega)$ also resembles the experimental one, where a broad maximum is found at 3.3 eV and a minimum at 4.3 eV.²³ A plot of $\epsilon(\omega)$ for the bulk material has been already presented and discussed in Ref. 19.

We have developed then a method to calculate optical properties starting from first-principles calculations. As the method is applied to calculate the dielectric function of bulk Si, good agreement is obtained between our values and the results available in the literature.²⁴ In the following section, we discuss the results of applying this method to study the optical properties of silicon clusters.

III. RESULTS AND DISCUSSION

We have calculated the electronic and optical properties of silicon clusters of 20, 60, and 70 atoms, with geometry configurations calculated in Ref. 5, and as briefly reviewed above. In Fig. 1, we show ideal (left), metastable (center), and equilibrium (right) configurations of Si_{20} , Si_{60} , and Si_{70} , respectively. Notice that the Si_{20} cluster does not have a fullerene-like metastable structure, and the equilibrium configuration is of a compact, closed-network type, which is 0.46 eV/atom more stable than the ideal fullerene geometry. On the other hand, it is found that metastable configurations of Si_{60} and Si_{70} do exist; these are fullerene-like, with warped bonding environments, but still retaining a hollow spherical shape. Notice, nevertheless, that the corresponding equilibrium geometries are of the network (compact) type.⁵ The Si_{60} (Si_{70}) equilibrium network is 0.33 (0.27) eV/atom more stable than the metastable fullerene-like configuration.

In the center column of Fig. 1 we can observe that metastable structures of Si_{60} and Si_{70} show the same atomic coordination as the corresponding ideal clusters (left column), composed by hexagons and pentagons. However, the metastable geometry is strongly distorted from the ideal configuration. In the right column of the figure one can see the increase on atomic coordination, resulting in the stabilization of dangling bonds introduced by the surface strains on ideal

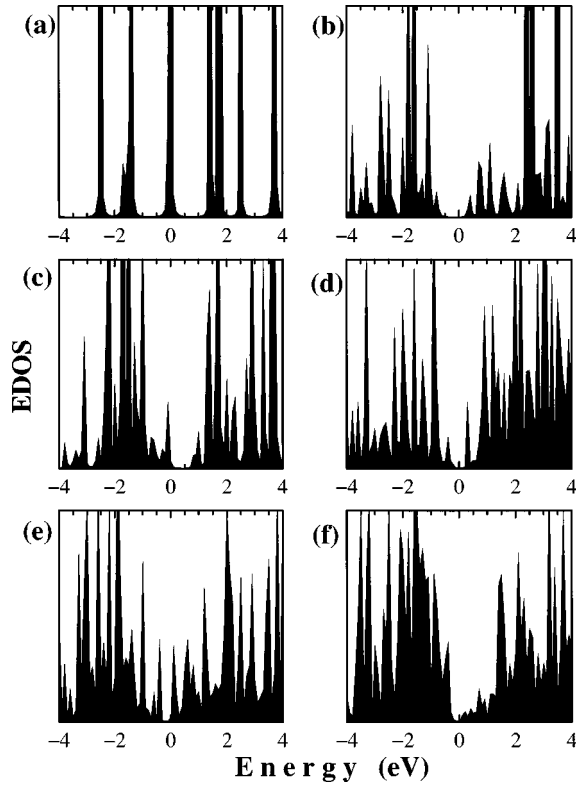


FIG. 2. EDOS of (a) ideal and (b) equilibrium configurations of Si_{20} ; (c) metastable and (d) equilibrium configurations of Si_{60} ; and (e) metastable and (f) equilibrium configurations of Si_{70} . The zero of EDOS corresponds to the calculated Fermi level, and a level broadening of 0.08 eV was used.

and metastable configurations. The fully relaxed (or annealed) silicon clusters do prefer a fourfold sp^3 -like coordination environment, although the finite size of the cluster results in even slight overcoordination (≈ 5) of the central atoms. Similar structural findings were reported in Ref. 25 for other cluster sizes.

A. Electronic structure

The vast structural differences among the various clusters, according to the number of atoms and energy, are directly reflected in their electronic and optical response. In Fig. 2, we show the electronic density of states (EDOS) corresponding to (a) the ideal Si_{20} , (b) network Si_{20} , (c) metastable Si_{60} , (d) network Si_{60} , (e) metastable Si_{70} , and (f) network Si_{70} clusters. The Fermi energy is at 0 eV and the curves have a level broadening of 0.08 eV. Notice that in the electronic levels shown for these clusters, we have not included LDA gap corrections as those used in the bulk crystal case. Therefore, the electronic gap of these systems is likely underestimated by about 0.6 eV.²⁶

In Fig. 2(a) for ideal Si_{20} , we observe a “metallic” behavior of the system, since electronic states are found right at the Fermi level (0 eV). On the other hand, a gap of about 1.2 eV is found for the equilibrium compact network structure. The EDOS of ideal Si_{20} is more sparse than the one found for the equilibrium configuration, as can be observed in Fig. 2(b). This fact might be attributed to the higher symmetry of ideal Si_{20} and, therefore, to the high degeneracy of the elec-

tronic states. Then, one would expect an optical spectrum for the ideal structure with features (peaks) associated with electron transitions that are more separated than for the spectrum of network Si_{20} .

In Figs. 2(c) and 2(d), we show the EDOS for metastable and equilibrium Si_{60} , respectively. We observe that the metastable structure has a larger gap (0.9 eV) than the corresponding one in the fully relaxed (annealed) “equilibrium” configuration (0.6 eV). Notice, moreover, that the density of empty states (those above 0 eV) for the equilibrium structure is larger at low energies than the density for the metastable one at such energies. This fact will also be reflected in the optical response, where one would expect a smoother profile of the dielectric function for the equilibrium structure than the one for the metastable configuration. Again, this behavior is expected since the symmetry of the metastable configuration is higher than the one of the equilibrium structure.

In Figs. 2(e) and 2(f), we show the EDOS for metastable and equilibrium Si_{70} clusters, respectively. We find the same behavior of the EDOS for the metastable and equilibrium configuration as that observed for the corresponding Si_{60} structures described above. However, the observed gaps for both configurations, metastable and equilibrium, show a reduction when the number of atoms increases from 60 to 70. For the metastable Si_{70} structure the gap is about 0.45 eV, while for the equilibrium one, the gap is slightly smaller at about 0.4 eV.

In general, we observe that the gap of the equilibrium or network structures is reduced as the number of atoms in the cluster increases. For the clusters with 60 and 70 atoms, we also observe that the gap of the metastable structures is larger than for the equilibrium configurations. It is also observed that the distribution of electronic states is more “sparse” when the system shows larger symmetry, as expected from the symmetry-induced degeneracies.

B. Optical spectra

The imaginary part of the dielectric function for these clusters was calculated according to Eq. (1). In Figs. 3, 4, and 5, we show the imaginary part of $\epsilon(\omega)$ of Si_{20} for the (a) ideal and (b) equilibrium configurations; and of Si_{60} and Si_{70} for the (a) metastable and (b) equilibrium configurations, respectively. In all figures, the dielectric response is shown for three different orthogonal polarizations (dot-dot, dash-dash, and dot-dash lines), and for their corresponding average (solid line). Notice also that a transition broadening of 0.05 eV has been added to smooth out the curves.

In Fig. 3(a), we observe the metallic behavior of the ideal Si_{20} cluster, since for small frequencies, $\omega \approx 0$, the intensity of $\text{Im}[\epsilon(\omega)]$ is very large compared with the rest of the spectrum. As pointed out above, the spectrum shows peaks that are separated between them, given by the discreteness of the electronic states. For example, the first two peaks correspond to electron transitions between states that are right below the Fermi level (around 0 eV) and the double structure above the Fermi level at about 1.6–1.8 eV. In this case, it is easy to identify the origin of the electronic transitions involved. One important characteristic of this optical spectra is that the re-

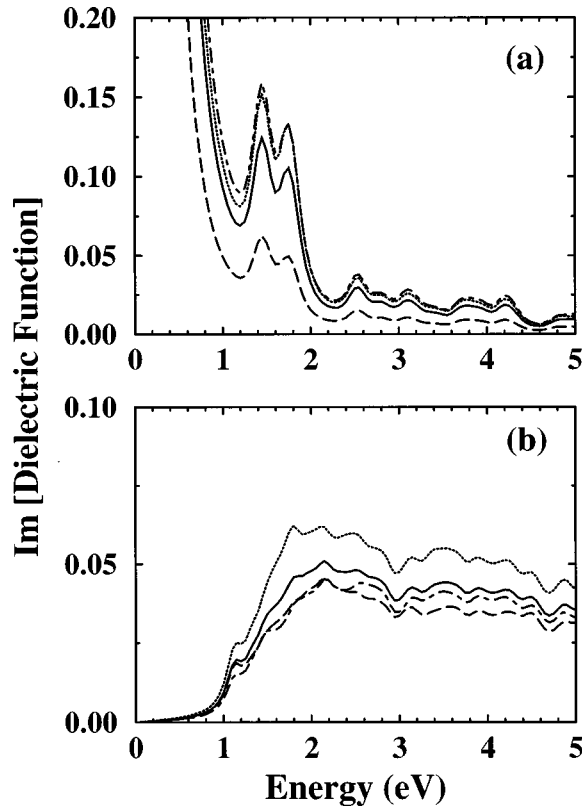


FIG. 3. Imaginary part of $\epsilon(\omega)$ for (a) ideal and (b) equilibrium configurations of Si_{20} . The solid line represents the average over three different light polarizations along x (dot-dot), y (dash-dash), and z (dot-dash) directions.

sponse along three different orthogonal directions is similar, varying only in intensity, and related to their overall isotropic geometry.

In Fig. 3(b), we show $\text{Im}[\epsilon(\omega)]$ for the fully relaxed (“equilibrium”) Si_{20} cluster. The large geometric difference between equilibrium and ideal configurations, is dramatically reflected in $\epsilon(\omega)$. While the ideal configuration shows a metalliclike behavior, a gap in the absorption spectra of about 1.2 eV is found for the equilibrium structure. It is remarkable that even after the equilibration process, the optical spectra are still nearly isotropic, varying only slightly in intensity. Moreover, the spectrum for the fully relaxed geometry lacks prominent peaks in the overall optical response, and a smoother and intense profile is found. We can clearly conclude that the relaxation process is accompanied by a breaking of electron degeneracies that are dramatically reflected in the optical response of the final structure. One would anticipate this to be a general result, from which the theoretical calculations would provide invaluable insights in comparison with experiments.

In Fig. 4, we show $\text{Im}[\epsilon(\omega)]$ of (a) metastable, and (b) fully relaxed Si_{60} clusters. The optical gap of 0.6 eV corresponding to the relaxed structure is two thirds that of the metastable configuration of 0.9 eV. In general, both spectra in Fig. 4 show a similar line shape, although the spectrum of the relaxed Si_{60} looks softer than the one for the metastable structure. However, the different atomic coordination of the equilibrium cluster leads to two new transitions at about 0.5 eV and 0.8 eV that do not appear in the metastable structure.

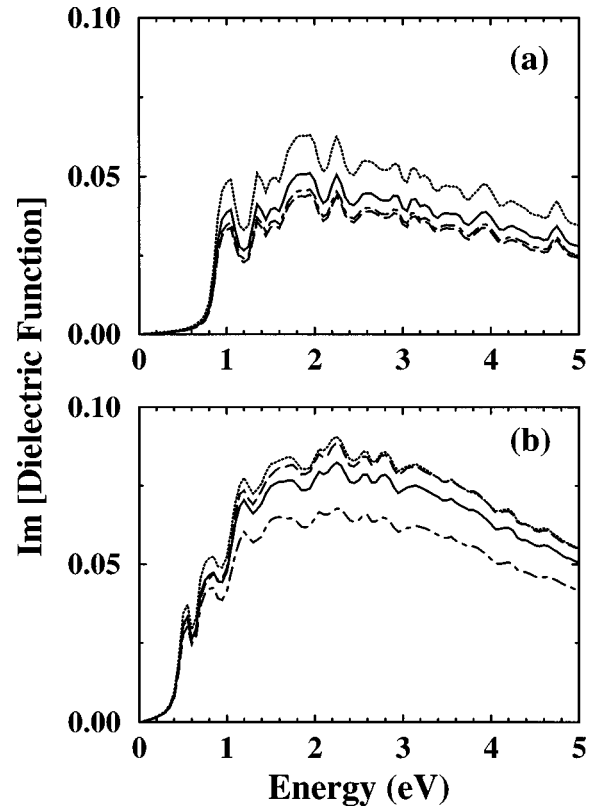


FIG. 4. Imaginary part of $\epsilon(\omega)$ for (a) metastable, and (b) equilibrium configurations of Si_{60} . The solid line represents the average over three different light polarizations along x (dot-dot), y (dash-dash), and z (dot-dash) directions.

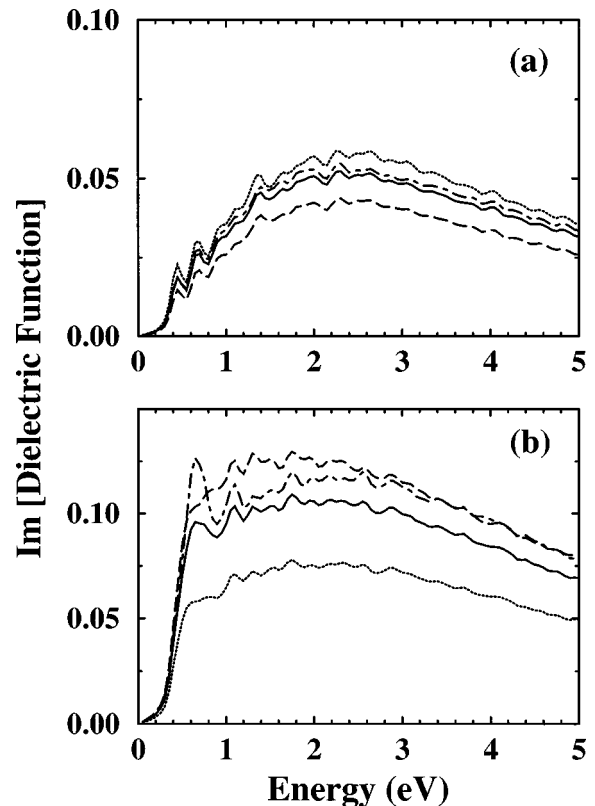


FIG. 5. Same as in Fig. 4 but for Si_{70} .

The presence of these strong features clearly differentiates the clusters. One important fact is that the optical response in both cases is still fairly isotropic, indicative of the overall symmetry of this cluster.

The energetic, as well as the electronic and optical properties of metastable and equilibrium configurations of Si_{70} appear, on a first look, to be similar to those described above for Si_{60} . In Fig. 5 we show $\text{Im}[\epsilon(\omega)]$ of (a) metastable, and (b) fully relaxed Si_{70} clusters. The gap of the metastable and equilibrium configurations are 0.45 eV and 0.40 eV, respectively. Like for the other clusters, the gap of equilibrium Si_{70} cluster is slightly smaller compared with the corresponding metastable Si_{70} . However, the difference in gap (and low-frequency excitations) between these two configurations is not as pronounced as in the previous examples. One important thing to notice in Fig. 5 is that the optical response of the equilibrium configuration is no longer isotropic. Notice, in particular, that at about 0.7 eV there is an electronic transition along one of the orthogonal directions (z , dot-dashed curve) that is more intense than in the rest of the spectra. This transition is basically absent in the spectra along the other two orthogonal directions, and especially along x (dotted curve). However, the rest of the spectra for the three orthogonal directions are still similar in shape, although not in intensity. This fact reflects a fundamental change due to the relaxation process, not only on the atomic configuration and coordination, but on the electronic structure as well. We also observe that, as for Si_{60} , the intensity of $\text{Im}[\epsilon(\omega)]$ for the equilibrium Si_{70} is larger than the one of the metastable structure at low energies. This is the result of an increased joint density of states for low excitations, as well as the smaller energy gap, produced by the massive level rearrangement accompanying the cluster relaxation.

IV. CONCLUSION

We have developed a first-principles method to calculate the optical properties of solids. This approach is not restricted to dealing with highly symmetric systems. The method allows one to study the optical properties of systems with large number of atoms (either total or per unit cell). Therefore, it is possible to study not only bulk structures, but other systems such as surfaces and large clusters as well. This is possible, in great measure, due to the fact that the method is based on a local-orbital basis set. As a first illustration of this method, we have calculated the electronic and optical properties of Si_{20} , Si_{60} , and Si_{70} clusters with different atomic configurations.

We have found that ideal, metastable, and fully relaxed geometries have different optical response that strongly depends on the atomic size of the cluster. We observe that the ideal Si_{20} configuration shows a metalliclike optical response, while the others show a gap in the excitation spec-

trum. The optical spectra for all metastable and relaxed cluster configurations show a gap of at least 0.4 eV. The gap in the relaxed structures decreases as the number of atoms in the cluster increases, perhaps the stronger remnant of quantum confinement of the electronic states for the smaller clusters. For energies below 5 eV, the intensity of $\text{Im}[\epsilon(\omega)]$ is larger for the relaxed structures than for metastable ones, due to the closing of the gap and accompanying level rearrangement. The profile of $\text{Im}[\epsilon(\omega)]$ in the equilibrium structures is “softer” than the one for ideal and metastable configurations, due to the breaking of structural symmetry. The optical response is nearly isotropic, indicating that the structural profile is similar for the three different orthogonal polarizations of light. Only for the largest cluster ($n=70$), this isotropic response is broken, and some anisotropy is found at low energies. We can observe that the relaxation process in all these clusters shows a dramatic change in the atomic coordination that is accompanied by a breaking of electron degeneracies for all the cluster structures.

The results presented here are in general agreement with experimental⁷ and theoretical⁸ observations of optical spectra for chains of silicon atoms. It has been found that the light absorption on these chains consisting of a small number of Si atoms ($n \leq 20$), occurs at larger energies than those with more atoms. When the number of atoms in the chains increases the energy absorption tends to a constant value ($n \geq 80$).⁷ Here, we find the same qualitative behavior in $\text{Im}[\epsilon(\omega)]$. The optical gap of the equilibrium Si_{20} cluster is about 0.6 eV larger than the one for Si_{60} , while this latter is only 0.1 eV larger than the gap of the relaxed Si_{70} cluster.

The inclusion of local field corrections (important in dense materials), as well as quasiparticle effects (which should be important in providing a detailed description of surface-localized states in solid surfaces), are the subject of our current efforts and will be presented elsewhere.²⁴ However, one would expect these effects to not be important for the clusters discussed here, and/or not affect our conclusions qualitatively.

ACKNOWLEDGMENTS

We want to especially thank J. Song who performed the atomic relaxation of the silicon clusters used here, and S. H. Yang who developed part of the QMD code that includes the d orbitals. A number of helpful discussions with D. A. Drabold are acknowledged. C.N. also acknowledges the support and hospitality of the Department of Physics and Astronomy at Ohio University, where most of the calculations were carried out. Finally, we acknowledge the partial support from Ohio University, CONACyT-Mexico Grant No. 900363-5-0075PE, and the Department of Energy Grant No. DE-FG02-91ER45334.

*Electronic address: cecilia@fenix.ifisicacu.unam.mx

¹R. Car and M. Parrinello, Phys. Rev. Lett. **55**, 2471 (1985).

²L. Kipp, D. K. Biegelsen, J. E. Northrup, L.-E. Swartz, and R. D. Bringans, Phys. Rev. Lett. **76**, 2810 (1996).

³C. Kress, A. I. Shkrebtii, and R. Del Sole, Surf. Sci **377-379**, 398 (1997).

⁴E. Kaxiras and K. Jackson, Phys. Rev. Lett. **71**, 727 (1993); J. C. Grossman and L. Mitás, *ibid.* **74**, 1323 (1995); K. D. Rinnen and M. L. Mandich, *ibid.* **69**, 1823 (1992); K. Fuke, K. Tsukamoto, F. Misaizu, and M. Sanekata, J. Chem. Phys. **99**, 7807 (1993).
⁵J. Song, S. E. Ulloa, and D. A. Drabold, Phys. Rev. B **53**, 8042 (1996).

- ⁶Y. Kanemitsu *et al.*, Appl. Phys. Lett. **61**, 2446 (1992).
- ⁷Y. Kanemitsu, K. Suzuki, Y. Nakayoshi, and Y. Masumoto, Phys. Rev. B **46**, 3916 (1992).
- ⁸M. S. Hybertsen and M. Needels, Phys. Rev. B **48**, 4608 (1993).
- ⁹See, e.g., *Light Emission from Silicon*, edited by S. S. Iyer, R. T. Collins, and L. T. Canham, MRS Symposia Proceedings No. 256 (Materials Research Society, Pittsburgh, 1992).
- ¹⁰P. V. Santos, B. Koopmans, N. Esser, W. G. Schmidt, and F. Bechstedt, Phys. Rev. Lett. **77**, 759 (1996).
- ¹¹O. F. Sankey and D. J. Niklewski, Phys. Rev. B **40**, 3979 (1989).
- ¹²D. R. Hamann, M. Schlüter, and C. Chiang, Phys. Rev. Lett. **43**, 1494 (1979).
- ¹³O. F. Sankey, D. J. Niklewski, D. A. Drabold, and J. D. Dow, Phys. Rev. B **41**, 12 750 (1990).
- ¹⁴O. F. Sankey *et al.*, Superlattices Microstruct. **10**, 407 (1991); G. B. Adams and O. F. Sankey, Phys. Rev. Lett. **67**, 867 (1991).
- ¹⁵D. R. Alfonso, C. Noguez, D. A. Drabold, and S. E. Ulloa, Phys. Rev. B **54**, 8028 (1996).
- ¹⁶R. W. Jansen and O. F. Sankey, Phys. Rev. B **36**, 6520 (1987); S. H. Yang, D. A. Drabold, J. B. Adams, P. Ordejon, and K. Glassford, J. Phys.: Condens. Matter **9**, L39 (1997).
- ¹⁷The improvement of electronic states occurs mostly on the empty levels, affecting little (if at all) the (meta)stable configurations obtained with the smaller basis.
- ¹⁸R. Del Sole, in *Photonic Probes of Surfaces*, edited by P. Halevi (Elsevier, Amsterdam, 1995), p. 148.
- ¹⁹C. Noguez, J. Song, S. E. Ulloa, D. A. Drabold, and S. H. Yang, Superlattices Microstruct. **20**, 405 (1996).
- ²⁰R. W. Godby, M. Schlüter, and L. J. Sham, Phys. Rev. B **37**, 10 159 (1988).
- ²¹See, for example, R. Del Sole and R. Girlanda, Phys. Rev. B **48**, 11 789 (1993).
- ²²The large number of k points in the calculation of the dielectric function is found to be necessary to deal with the strongly parallel bands, yielding large contributions to the joint density of states in bulk silicon.
- ²³M. L. Cohen and J. R. Chelikowsky, *Electronic Structure and Optical Properties of Semiconductors*, Springer Series in Solid-State Sciences Vol. 75 (Springer-Verlag, New York, 1989).
- ²⁴The rather good agreement with experiment is somewhat surprising, as our approach does not include local field effects [see, e.g., W. L. Mochán and R. G. Barrera, Phys. Rev. Lett. **55**, 1192 (1985); **56**, 2221 (1986)]; and many-body corrections [see, e.g., M. S. Hybertsen and S. G. Louie, Phys. Rev. B **34**, 5390 (1986)]. Although the calculation does not yield the excitonic features, the rest of the function is reproduced quite well, perhaps due to fortuitous cancellation effects.
- ²⁵U. Röthlisberger, W. Andreoni, and M. Parrinello, Phys. Rev. Lett. **72**, 665 (1994).
- ²⁶It is well known that the electronic gap of bulk Si calculated by LDA, is underestimated by 0.6 eV.